American Journal of Biomedical Sciences
ISSN: 1937-9080
nwpii.com/ajbms

Simultaneous Gas-phase Detection of Nitric Oxide (NO) and Nitrous Oxide (N_2O) from the Decomposition of Angeli's Salt ($Na_2N_2O_3$) at Different pHs Using Tunable-diode Laser Absorption Spectroscopy

Jun Yi [a], Khosrow Namjou [b], Patrick J. McCann [c], and George B. Richter-Addo [a,*]

[a] Department of Chemistry and Biochemistry, University of Oklahoma, 620 Parrington Oval, Norman, Oklahoma, U.S.A., 73019
[b] *Ekips Technologies Inc., 710 Asp Avenue, Norman, OK, 73069*
[c] *School of Electrical and Computer Engineering, University of Oklahoma, 202 West Boyd St., Norman, Oklahoma, U.S.A., 73019*
***Corresponding Author:**
George B. Richter-Addo
Tel.: +1 405 325 6401; fax: +1 405 325 6111.
E-mail address: grichteraddo@ou.edu

Received: 16 October 2008; | Revised: 25 November 2008; | Accepted: 28 November 2008

Abstract

Nitric oxide (NO) is a gaseous diatomic molecule that is biosynthesized in mammals, and it regulates a host of physiological processes including blood pressure. Over the last several years, there has been an increased interest in the redox partner HNO and its identifiable dimerization product N_2O. This latter gaseous species is also the product of various NO-coupling reactions as occurs in bacterial NO-detoxification processes. An attractive new tool will be the ability to simultaneously detect NO and N_2O from the same reaction vessel. We demonstrate proof-of-concept methodology for such a simultaneous and specific NO and N_2O detection from the same precursor (from Angeli's salt decomposition) using tunable diode laser absorption spectroscopy without the need for separation or pretreatment of these gases.

Keywords: Nitric oxide; Nitrous oxide; detection; TDLAS; Angeli's salt

1. Introduction

Several small molecule oxides of nitrogen (N-oxides) are biologically relevant. Denitrifying bacteria convert nitrate to dinitrogen in a series of steps that involve distinct metalloenzymes for each step [1]. Nitrate reductase enzymes convert nitrate (NO_3^-) to nitrite (NO_2^-). Nitrite is then converted to nitric oxide (NO) by the dissimilatory nitrite reductase enzymes. The reduction of NO to nitrous oxide (N_2O) is carried out by the bacterial NO reductase enzymes [2] (a fungal NO reductase enzyme also exists [3]), followed by N_2O conversion to dinitrogen by the nitrous oxide reductase enzyme.

NO is biosynthesized in mammals by the NO synthase enzymes, and NO serves as a signaling agent towards the enzyme soluble guanylyl

cyclase to result in vasodilation. Recently, evidence has been presented to demonstrate that NOS can also produce HNO (nitroxyl) under some conditions [4, 5]. There is increased interest in the development of HNO-based drugs for the treatment of cardiac failure [6, 7], and the biological action of HNO has been shown to be quite different from that of NO [8, 9]. Interestingly, HNO is converted to NO upon reaction with ferric hemes [10-12] and with Cu,Zn-SOD [13, 14]. HNO, however, also rapidly dimerizes to N_2O (with water as a byproduct) with a rate constant of 8×10^6 M^{-1} s^{-1} [15]. Indeed, it is N_2O that was measured in the NOS studies implicating HNO as a primary product of NO synthase activity [5]. In general, for convenience, N_2O is frequently used as a reliable marker for HNO, and the N_2O is detected using infrared spectroscopy, gas chromatography (GC), or GC-mass spectrometry (GC-MS) [16, 17]. The latter methods, however, require the use of specialized columns for the separation of N_2O (*m/z* 44) from CO_2 (*m/z* 44).

We are interested in the mammalian biochemistry of the simple N-oxides involving heme-HNO, heme-nitrite, and heme-NO derivatives. During our work, we were surprised to learn that there were no reports for the direct and *simultaneous* measurements of NO and N_2O generated from a chemical or biological system. In an effort to develop methodology that will enable such a simultaneous detection, we selected as a prototype the decomposition of the well-known Angeli's salt (disodium trioxodinitrate, $Na_2N_2O_3$) [18-20]. Angeli's salt is known to generate HNO at physiological pH. However, it also generates NO at low pH. This pH-dependent decomposition to NO and/or HNO was attractive as a prototypical system, and we reasoned that the results obtained from the simultaneous detection should provide a pH-dependent profile of released NO/N_2O under the same experimental reaction conditions.

We recently reported the direct and specific detection of NO and its ^{15}NO isotope using tunable-diode laser absorption spectroscopy (TDLAS) without the need for mass spectroscopy [21]. Fritsch et al. have recently also reported the use of infrared cavity leak-out spectroscopy for the quantification of NO [22]. We reasoned that with the appropriate instrument modification, and given the above-mentioned differential production of NO or N_2O from Angeli's salt decomposition, that we should be able to perform a *simultaneous* specific and direct detection of both NO and N_2O without the need for pretreatment or separation of these gases. We are pleased to report our successful demonstration of proof-of-principle for this simultaneous direct and specific NO/N_2O detection from the same sample in real time and/or as accumulated gases.

2. Experimental Section

Angeli's salt was purchased as a solid from Caymen Chemical (Ann Arbor, MI, USA) and stored at –20 ℃ to minimize decomposition. Freshly prepared stock solutions of Angeli's salt were made in 10 mM degassed NaOH. DTPA (diethylenetriamine-pentaacetic acid) was purchased from TCI America. Citric acid (Merck), KCl (Fisher Scientific), glycine (>98.5%, Fisher Scientific), and Tris-HCl (>99%, Fluka) were purchased from commercial sources. The respective 100 mM buffers were prepared in distilled and deionized water, and then degassed. The buffers were selected based on the table of buffer pHs from the Hampton Research catalog, and their pHs checked before and after the measurements in this work; the variations were typically ±0.1 units. In a typical experiment for the pH dependence study, an air-tight syringe was used to inject 0.5 mL of degassed Angeli's salt stock solution (containing 500 μM of DTPA to scavenge trace metal ions) into 5.0 mL of a previously degassed 100 mM buffer solution to initiate the decomposition reaction. Each reaction was performed in at least duplicate.

2.1 Instrumentation and detection of NO and N_2O

NO and N_2O detection is based on high-resolution tunable diode laser absorption spectroscopy (TDLAS). TDLAS is a well known and proven method for the direct measurements of important trace gases [23]. The experimental setup is shown in Figure 1. We have previously described a similar setup for the NO detection methodology [21]; the new setup has a gas splitter placed just after the output from the sample chamber, and the overall set consists of duplicate

components of that shown in Figure 1 (except the single sample chamber). For convenience, only one of these duplicate TDLAS setups is shown in the figure. Briefly, the cold head in the vacuumed cryostat housing contains one or two IV-VI semiconductor tunable diode laser sources emitting in the mid-infrared spectral region around 4.6 μm (for N_2O detection) or 5.2 μm (for NO detection). The diverging laser output beam is first collimated using an off-axis-parabolic (OAP) mirror and directed through an astigmatic multipass Herriott cell where the beam passes through the sample gas over a path of 36 meters for the infrared absorption measurements. We utilized, for convenience, a 100 meter optical pathlength for the N_2O measurements in our experiments. The laser beam, upon exiting the cell, is focused using a ZnSe lens onto an HgCdTe photodetector located inside the sealed vacuum housing. Both the laser and the mid-IR photodetector are cryogenically cooled with either a single-stage closed cycle refrigerator or a Stirling engine cooler; this allows a liquid-nitrogen-free operation of the instrumentation. The signal detection performs through a wavelength modulation scheme. The laser wavelength is tunable with heat-sink temperature or driving current. For the gas sensing experiments with the TDLAS system, the Herriott cell was evacuated to reduce the pressure to 2.2–2.5 Torr prior to the introduction of the produced gas from the sample chamber into the cell. This allows more efficient transfer of the gas from the sample chamber to the Herriott cell. For real-time measurements, an oil-free diaphragm pump and a precise gas flow controller (Alicat Scientific, AZ) were used to hold the pressure in the Herriott cell down to 45 Torr to reduce pressure-broadening effects on absorption profile lines, and to allow controlled gas flow through the glassware at a set value of 1 L per minute. The glassware is a slight modification of a design previously reported [21].

High-resolution absorption measurements are achieved by scanning the laser wavelength over the absorption features of NO from 1914.80 to 1915.72 cm^{-1}, and N_2O from 2198.40 to 2199.04 cm^{-1}. We utilized data contained in the HITRAN 1996 database [24] to select the appropriate spectral regions for study. Figure 2 shows the laser absorption spectra of measured NO and N_2O and the corresponding HITRAN lines that were used to identify these gases. The H_2O lines in the spectra were used for spectral centering. The absorption peaks chosen were the split peaks at 1914.98/1914.99 cm^{-1} for NO and 2198.995/2199.016 cm^{-1} for N_2O. The latter smaller intensity peaks for N_2O were chosen over the larger intensity peak at 2198.720 cm^{-1} (Figure 2, right) so as not to saturate the absorption signals during the measurements.

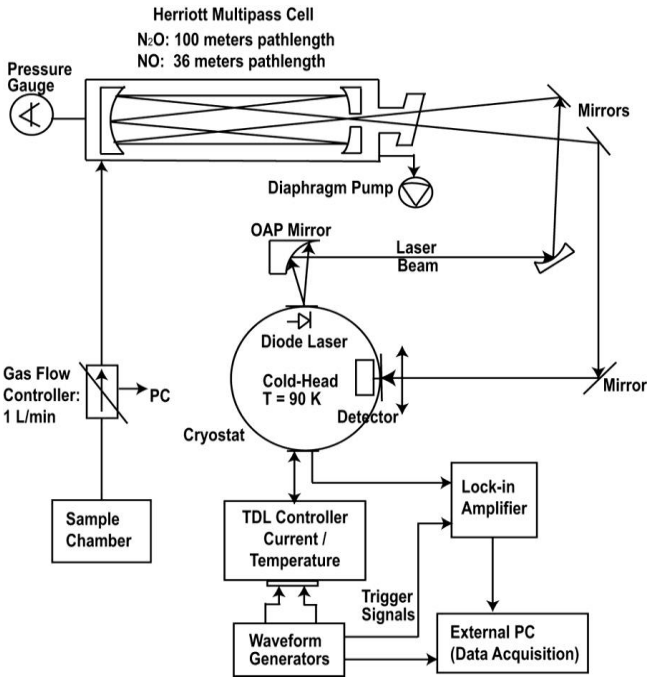

Fig. 1 Schematic diagram of the TDLAS instrument. A splitter is placed after the sample chamber, and only one of the duplicate systems is shown. Major components for each system include a cryostat, Herriott multipass cell, and an integrated gas sampling interface.

As expected, the measured absorption intensities are proportional to the concentrations of NO and N_2O in the sample chamber. We have shown previously that a direct linear correlation exists between absorption intensity and NO concentrations in the 0-500 ppb range [25]. A similar direct linear correlation exists for N_2O up to 10 ppm (using the smaller doublet peaks at 2198.995/2199.016 cm^{-1}; Figure 2). In this current study, the NO calibration utilized a standard 1 ppm solution of NO in N_2. The N_2O calibration

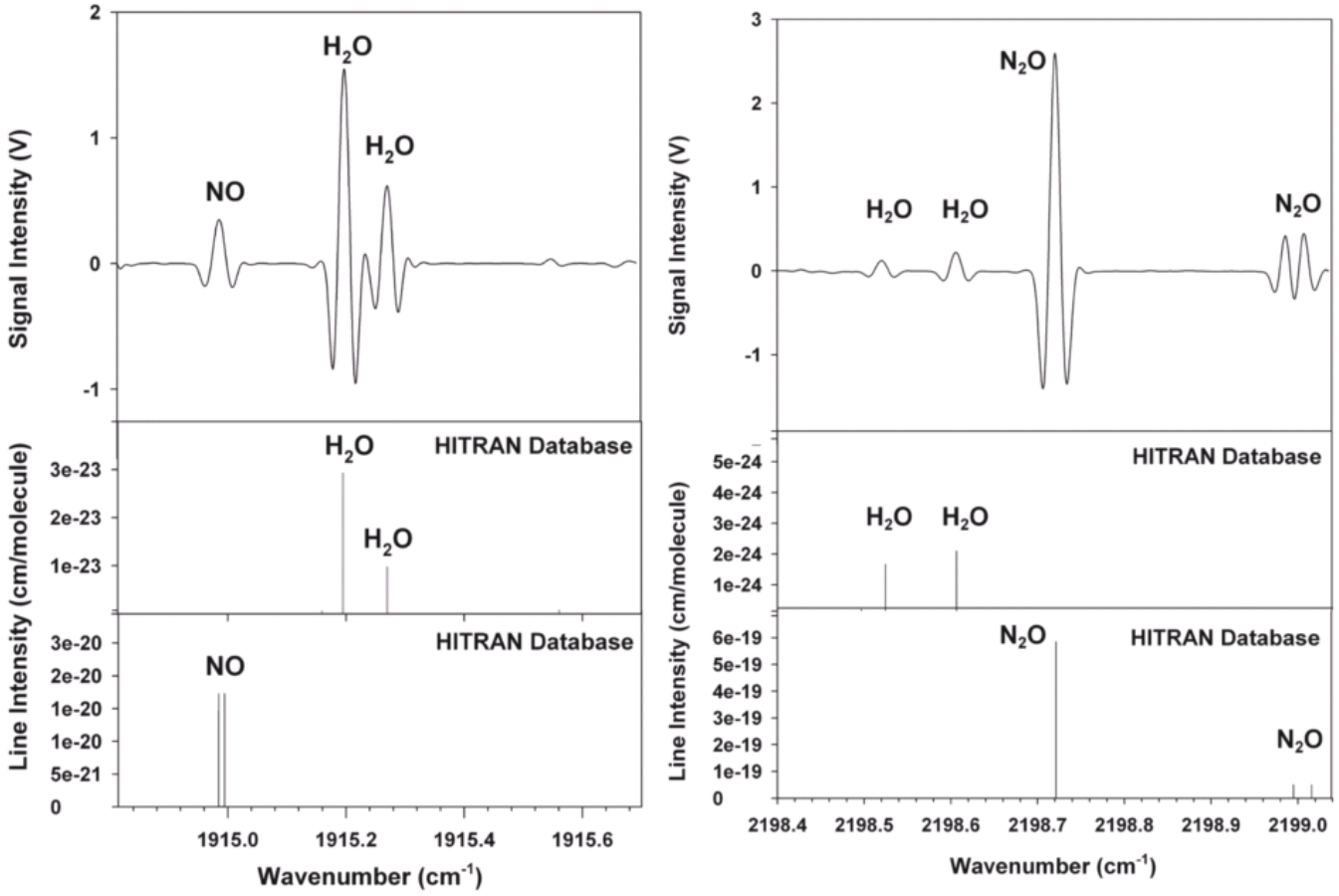

Fig. 2 (*Left*) Second-harmonic spectrum of measured NO from ambient air (upper), corresponding line intensities (in cm^{-1}/ molecule $\times cm^{-2}$) and frequencies of H_2O (middle) and NO (bottom) from 1914.80 to 1915.72 cm^{-1} found in the HITRAN 1996 database. (*Right*) Corresponding data for N_2O in the spectral range 2198.40 to 2199.04 cm^{-1}.

utilized both 1 ppm and 10 ppm (in N_2) standards. The NO and N_2O responses were recorded in volts.

3. Results and Discussion

A superior advantage of the mid-infrared tunable diode laser absorption spectroscopy (mid-IR TDLAS) methodology for the identification of NO and N_2O is the ability to specifically and directly detect these gases without interference of signals from other species in the gaseous mixtures. For example, IR detection of NO and N_2O at 1880 cm^{-1} [26] and 2224 cm^{-1} [27], respectively, has been employed in many bulk scale chemical reactions involving these gases. However, the TDLAS methodology allows for the selection of any of several absorption bands that do not overlap with the IR absorption peaks of other species that may absorb in the regions of interest. Figure 2 illustrates the case where, within the narrow range of 2198.4–2199 cm^{-1}, four absorption features can be located, two for H_2O and two for N_2O (the higher energy absorption for N_2O being a split band).

To the best of our knowledge, no methods that describe the simultaneous direct detection of NO and N_2O from chemical reaction mixture have been reported. Our results demonstrate a proof-of-concept for both the real-time detection of these gases and the semi-quantitative assessment of the ratio of NO and N_2O production from the same reaction mixtures without the need for separation of the gaseous products. We selected the well-known Angeli's salt ($Na_2N_2O_3$) decomposition reaction as our experimental model due to the fact

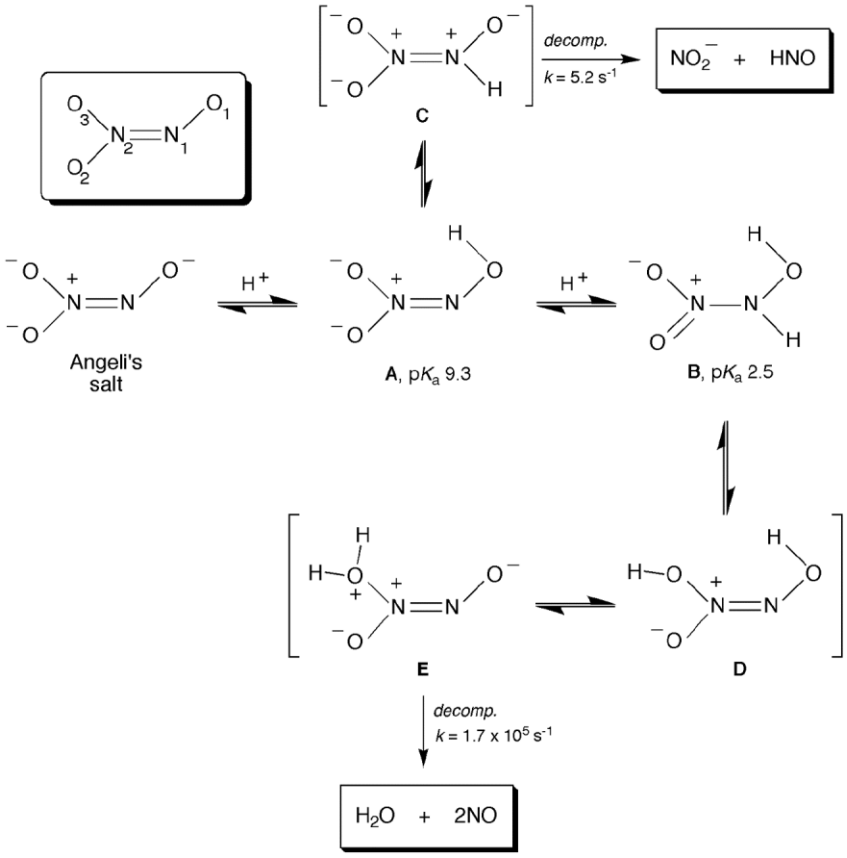

Scheme 1

that it releases NO and/or N_2O depending on the pH of the reaction medium.

The p*K*as for the protonated form of Angeli's salt, namely oxyhyponitrous acid $H_2N_2O_3$, are 2.5 and 9.7 [28]. It has been reported that the rate of aqueous decomposition of Angeli's salt is pH independent in the pH 4–8 range [19]. At physiological pH, the salt decomposes into HNO and nitrite; at very low pH, NO is the predominant gaseous product generated as determined by mass spectrometry [19]. Theoretical calculations by Houk and coworkers [29] have provided mechanistic insight into the site(s) of protonation of Angeli's salt that lead to the different nitrogen oxide products (Scheme 1). Thus, at physiological pH, the O1 atom of the dibasic Angeli's Salt is initially protonated to form the monoprotonated species **A** (Scheme 1) with a calculated p*K*a of 9.3. This unreactive species will be in equilibrium with a reactive intermediate **C** which will homolytically cleave the N-N bond to form HNO and nitrite ion with a rate constant of 5.2 s^{-1}. At low pH, a second proton will attack at the N1 atom of species **A** to form the diprotonated species **B** with a calculated p*K*a of 2.5. This unreactive intermediate will be in equilibrium with species **D** followed by an intramolecular proton transfer to form a reactive intermediate **E** which decomposes to H_2O and NO with with a rate constant of 1.7×10^5 s^{-1}. There have been several reports that confirm the production of NO from the low pH decomposition of Angeli's salt and HNO/N_2O production at pH values higher than 4 [9, 16, 17, 30]. A clear advantage of a possible simultaneous NO and N_2O measurement would be the ability to perform both real-time monitoring of these gases and the determination of the relative ratios of NO and N_2O produced under different pH conditions.

In our experiments, the real-time measurements of N_2O and NO were performed similarly. We previously reported the description for the real time NO measurements [21]. In the

case of the real-time N_2O measurements, extra precaution must be taken to assess the contributions of ambient N_2O to the absorption signals. To illustrate the importance of this consideration, we show in Figure 3 the effect of ambient air on the N_2O detection response. The sample and detection chambers were allowed initially to equilibrate at 45 torr with a supplemental nitrogen gas flow. Opening the empty sample chamber to laboratory air while shutting off the supplemental nitrogen gas flow resulted in a spike in N_2O detection (labeled (a) in the Figure). Resealing the system restored the baseline. Angeli's salt was then added to the sample chamber by opening the chamber and introducing the solid; the spike in N_2O detection (labeled (b) in the Figure) is due to the ambient air. Upon addition of the degassed buffer to initiate the aqueous decomposition of the salt, a large N_2O response (labeled (c) in the Figure) became evident which then trailed to near-baseline levels over time. These N_2O response features are reproducible.

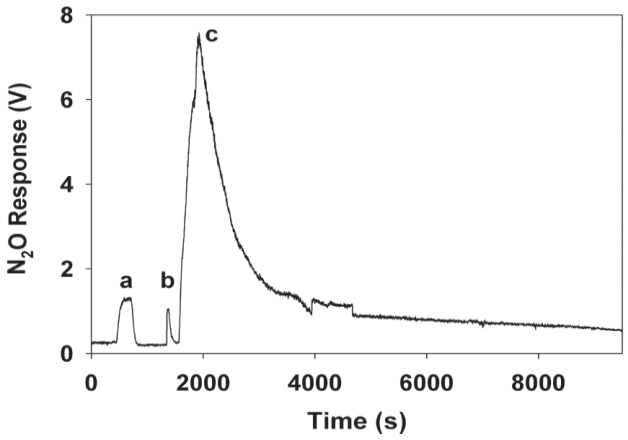

Fig. 3 Real-time measure of N_2O from the decomposition of Angeli's salt in 100 mM Tris-HCl buffer containing 50 μM DTPA at pH 7.4. (a) The sample chamber was open to air and then re-sealed. (b) The sample chamber was opened to introduce 2 mg of Angeli's salt as a solid, and then re-sealed. (c) The N_2O produced after 5 mL of the degassed buffer was delivered to the Angeli's salt in the sample chamber. The apparent noisy feature around 4000-4400 sec is due to manual electronic adjustments during the data collection.

As mentioned previously, the rate of Angeli's salt decomposition in aqueous solution (i.e., rate of disappearance of the salt in solution) is pH independent in the pH 4–8 range [19, 31]. However, there does not appear to be any report on the relative ratios of the N_2O and NO gases generated as a function of pH. In order to provide a semi-quantitative measurement regarding the ratio of NO and N_2O produced from the aqueous Angeli's salt decomposition reactions in the pH 2.0–9.4 range, we allowed the decompositions to run for a maximum of 16 h in a sealed vessel to insure completion of the reactions. An independent time course measurement for N_2O production at pH 7.4 revealed a period of 7 h for the reaction to go to near-completion (data not shown). The headspace was then simultaneously analyzed for NO and N_2O after this period using the TDLAS system. Similar timeframes have been employed by other researchers for monitoring Angeli's salt decompositions (e.g., 22 h at pH 8.5) [31] and for N_2O measurements from nitrosothiol/thiol reactions (24 h)[32]. The relative ratios of NO and N_2O detected from Angeli's salt decomposition (this work) in the pH 2.0–9.4 range using our TDLAS-based system are shown in Figure 4.

There are several points to note from the data in Figure 4. Before discussing these, however, an important point needs to be addressed (Scheme 2). Studies of Angeli's salt decomposition have been

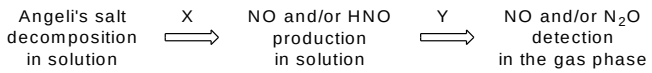

Scheme 2

reported previously, including measurements of the rates of decomposition (e.g., disappearance of UV-vis spectral markers for the salt; left of Scheme 2) in solution [19, 31]. The effects of added reagents such as oxygen and nitrite (labeled X) on Angeli's salt decomposition to give varied amounts of NO and/or HNO or other species have also been reported (middle of Scheme 2) [19, 33]. A common and reasonable assumption is that all the N_2O detected (right side of Scheme 2) during Angeli's salt decomposition results from the HNO generated initially. A proposed role of buffer as

species Y is discussed later. The use of Angeli's salt in this proof-of-concept project is to demonstrate the simultaneous detection of NO/N_2O (right side of Scheme 2) from the decomposition of the salt, and not to further explore the detailed mechanism of Angeli's salt decomposition (left of Scheme 2) or the effects of added reagents (X and Y in Scheme 2).

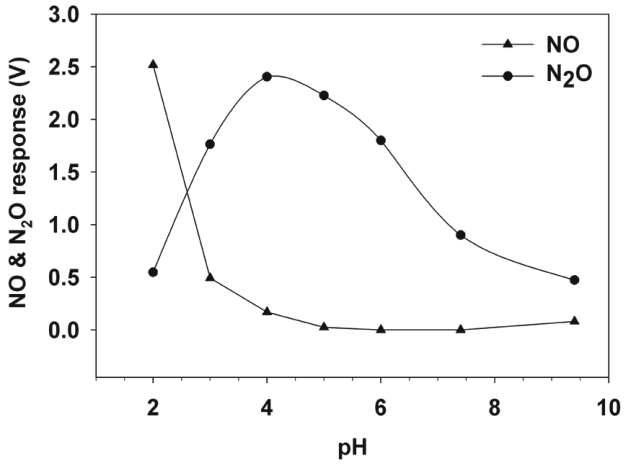

Fig. 4 Simultaneous detection of NO (triangles) and N_2O (dots) release from the decomposition of Angeli's salt under different pH conditions. Buffers used for pH control: 100 mM KCl (pH 2.0), 100 mM citric acid (pH 3.0, 4.0, 5.0, and 6.0), 100 mM Tris HCl (pH 7.4), and 100 mM glycine (pH 9.4). For these reactions, 0.50 mL of a freshly made stock 2.4 mM Angeli's salt solution containing 500 μM DTPA was injected to each of 5.0 mL of the degassed buffers to make the final concentration of AS 0.22 mM, respectively.

Returning to Figure 4, we find that the amount of NO detected sharply increases below pH 3 (high acidity), and this is correlated with its known generation in this pH range [19]. Second, the amount of N_2O detected from our experiments is maximum at pH 4, and declines sharply at higher acidity as the amount of NO detected increases. Third, the amount of N_2O detected at pH>4 declines without an associated increase in the amount of NO detected. In addition, there is a slight increase in the NO response at pH 9.4.

It is generally accepted that NO generation from Angeli's salt is not favored at pH>4. However, we note that the N_2O *detection* profile in Figure 4 (right of Scheme 2) varies slightly from the previously reported Angeli's salt *decomposition* profile (left of Scheme 2) which shows a steady pH-independent decomposition rate between pH 4.5–8 and a sharp decrease in rate of decomposition at pH>9 [31]. Although we are not certain about the reason for the drop in N_2O *detection* at high pH values, this could be due to the fact that the nitroxyl anion $^3NO^-$ predominates over HNO (hence N_2O) at high pH values, and the chemistry of NO/HNO mixtures can be complicated further by the known hydroxide anion-catalyzed reaction between NO and HNO [15]. Further, Miranda and coworkers have suggested a possible interaction between reactive intermediates of Angeli's salt decomposition with the unprotonated amine form of HEPES buffer [34]; we utilized Tris (pK_a 8.3) and glycine (pK_a 9.6) for our measurements at pH 7.4 and 9.4, respectively. Our real-time and cummulative NO/N_2O simultaneous detection methodology allows further opportunities to explore the use of this salt as an HNO/N_2O donor under different buffer conditions. For example, will the amount of available HNO produced by Angeli's salt decomposition be affected the choice of buffer used (Y in Scheme 2) prior to its dimerization to N_2O? We plan to examine such questions for various known HNO donors in the near future.

In summary, we report the first simultaneous and specific detection of NO and N_2O from a liquid-phase reaction mixture, without the need for prior separation or pretreatment of these gases. Importantly, we expect this TDLAS-based methodology to be applicable to other NO/N_2O generating systems such as those found in natural NO-detoxification processes (e.g., NO-reductase enzymes) where simultaneous semi-quantitative measurements of NO consumption and N_2O production in headspace gases can be monitored from the same sample. The system is flexible to allow for very small sample volumes for enzyme work.

Acknowledgements

We are grateful to the National Institutes of Health (GM64476: GBR-A) for funding for this research.

References

1. Eady, R. R.; Hasnain, S. S. *Denitrification*, in Comprehensive Coordination Chemistry II, L. Que Jr. and W. B. Tolman, eds. Elsevier, San Diego, CA 2004, pp. 759-786.
2. Zumft, W. G.; Nitric Oxide Reductases of Prokaryotes with Emphasis on the Respiratory, Heme-Copper Oxidase Type, *J. Inorg. Biochem.*, 2005, 99, 194-215.
3. Daiber, A.; Shoun, H.; Ullrich, V.; Nitric Oxide Reductase (P450nor) from *Fusarium oxysporum*, *J. Inorg. Biochem.*, 2005, 99, 185-193.
4. Rusche, K. M.; Spiering, M. M.; Marletta, M. A.; Reactions Catalyzed by Tetrahydrobiopterin-Free Nitric Oxide Synthase, *Biochemistry*, 1998, 37, 15503-15512.
5. Ishimura, Y.; Gao, Y. T.; Panda, S. P.; Roman, L. J.; Masters, B. S. S.; Weintraub, S. T.; Detection of Nitrous Oxide in the Neuronal Nitric Oxide Synthase Reaction by Gas Chromatography-Mass Spectrometry, *Biochem. Biophys. Res. Commun.*, 2005, 338, 543-549.
6. Feelisch, M.; Nitroxyl Gets to The Heart of The Matter, *Proc. Natl. Acad. Sci., USA*, 2003, 100, 4978-4989.
7. Paolocci, N.; Katori, T.; Champion, H. C.; St. John, M. E.; Miranda, K. M.; Fukuto, J. M.; Wink, D. A.; Kaas, D. A.; Positive Inotropic and Luitropic Effects of HNO/NO^- in Failing Hearts: Independence from β-Adrenergic Signaling, *Proc. Natl. Acad. Sci., USA*, 2003, 100, 5537-5542.
8. Miranda, K. M.; Paolocci, N.; Katori, T.; Thomas, D. D.; Ford, E.; Bartberger, M. D.; Espey, M. G.; Kaas, D. A.; Feelisch, M.; Fukuto, J. M.; Wink, D. A.; A Biochemical Rationale for the Discrete Behavior of Nitroxyl and Nitric Oxide in the Cardiovascular System, *Proc. Natl. Acad. Sci., USA*, 2003, 100, 9196-9201.
9. Miranda, K. M.; Ridnour, L.; Esprey, M.; Citrin, D.; Thomas, D.; Mancardi, D.; Donzelli, S.; Wink, D. A.; Katori, T.; Tocchetti, C. G.; Ferlito, M.; Paolocci, N.; Fukuto, J. M.; Comparison of the Chemical Biology of NO and HNO: An Inorganic Perspective, *Prog. Inorg. Chem.*, 2005, 54, 349-384.
10. Bazylinski, D. A.; Hollocher, T. C.; Metmyoglobin and Methemoglobin as Efficient Traps for Nitrosyl Hydride (Nitroxyl) in Neutral Aqueous Solution, *J. Am. Chem. Soc.*, 1985, 107, 7982-7986.
11. Suarez, S. A.; Marti, M. A.; De Baise, P. M.; Estrin, D. A.; Bari, S. E.; Doctorovich, F.; HNO Trapping and Assisted Decomposition of Nitroxyl Donors by Ferric Hemes, *Polyhedron*, 2007, 26, 4673-4679.
12. Bari, S. E.; Martf, M. A.; Amorebieta, V. T.; Estrin, D. A.; Doctorovich, F.; Fast Nitroxyl Trapping by Ferric Porphyrins, *J. Am. Chem. Soc.*, 2003, 125, 15272-15273.
13. Murphy, M. E.; Sies, H.; Reversible Conversion of Nitroxyl Anion to Nitric-Oxide by Superoxide-Dismutase, *Proc. Natl. Acad. Sci. USA*, 1991, 88, 10860-10864.
14. Liochev, S. I.; Fridovich, I.; Copper,Zinc Superoxide Dismutase as a Univalent NO^- Oxidoreductase and as a Dichlorofluorescin Peroxidase, *J. Biol. Chem.*, 2001, 276, 35253-35257.
15. Shafirovich, V.; Lymar, S. V.; Nitroxyl and Its Anion in Aqueous Solutions: Spin States, Protic Equilibria, and Reactivities Towards Oxygen and Nitric Oxide, *Proc. Natl. Acad. Sci. USA*, 2002, 99, 7340-7345.
16. Miranda, K. M.; The Chemistry of Nitroxyl (HNO) and Implications in Biology, *Coord. Chem. Rev.*, 2005, 249, 433-455.
17. Wink, D. A.; Feelisch, M. *Formation and Detection of Nitroxyl and Nitrous Oxide*, in Methods in Nitric Oxide Research, M. Feelisch and J. S. Stamler, eds. John Wiley & Sons Ltd., Chichester 1996, pp. 403-412 (Chapter 28).
18. Miranda, K. M.; Dutton, A. S.; Ridnour, L. A.; Foreman, C. A.; Ford, E.; Paolocci, N.; Katori, T.; Tocchetti, C. G.; Mancardi, D.; Thomas, D. D.; Espey, M. G.; Houk, K. N.; Fukuto, J. M.; Wink, D. A.; Mechanism of Aerobic Decomposition of Angeli's Salt (Sodium Trioxodinitrate) at Physiological pH, *J. Am. Chem. Soc.*, 2005, 127, 722-731.
19. Hughes, M. N.; Wimbledon, P. E.; The Chemistry of Trioxodinitrates. Part 1.

Decomposition of Sodium Trioxodinitrate (Angeli's Salt) in Aqueous Solution, *J. Chem. Soc., Dalton Trans.*, 1976, 703-707.
20. Hughes, M. N.; Cammack, R.; Synthesis, Chemistry, and Applications of Nitroxyl Ion Releasers Sodium Trioxodinitrate or Angeli's Salt and Piloty's Acid, *Methods Enzymol.*, 1999, 301, 279-287.
21. Yi, J.; Namjou, K.; Zahran, Z. N.; McCann, P. J.; Richter-Addo, G. B.; Specific Detection of Gaseous NO and ^{15}NO in the Headspace from Liquid-Phase Reactions Involving NO-Generating Organic, Inorganic, and Biochemical Samples using a Mid-Infrared Laser, *Nitric Oxide*, 2006, 15, 154-162.
22. Fritsch, T.; Brouzos, P.; Heinrich, K.; Kelm, M.; Rassaf, T.; Hering, P.; Kleinbongard, P.; Murtz, M.; NO Detection in Biological Samples: Differentiation of ^{14}NO and ^{15}NO using Infrared Laser Spectroscopy, *Nitric Oxide*, 2008, 19, 50-56.
23. Werle, P.; A Review of Recent Advances in Semiconductor Laser Based Gas Monitors, *Spectrochim Acta*, 1998, 54A, 197-236.
24. Rothman, L. S.; Rinsland, C. P.; Goldman, A.; Massie, S. T.; Edwards, D. P.; Flaud, J.-M.; Perrin, A.; Camy-Peyret, C.; Dana, V.; Mandin, J.-Y.; Schroeder, J.; McCann, A.; Gamache, R. R.; Wattson, R. B.; Yoshino, K.; Chance, K. V.; Jucks, K. W.; Brown, L. R.; Nemtchinov, V.; Varanasi, P.; The HITRAN Molecular Spectroscopic Database and HAWKS (HITRAN ATMOSPHERIC WORKSTATION): 1996 Edition, *J. Quant. Spectrosc. Radiat. Transfer*, 1998, 60, 665-710.
25. Roller, C.; Namjou, K.; Jeffers, J. D.; Camp, M.; Mock, A.; McCann, P. J.; Grego, J.; Nitric Oxide Breath Testing by Tunable-Diode Laser Absorption Spectroscopy: Application In Monitoring Respiratory Inflammation, *Applied Optics*, 2002, 41, 6018-6029.
26. Richter-Addo, G. B.; Legzdins, P., *Metal Nitrosyls*, Oxford University Press, New York, 1992.
27. Burch, D. E.; Williams, D.; Total Absorptance by Nitrous Oxide Bands in the Infrared, *Appl. Optics*, 1962, 1, 473-482.
28. Sturrock, P. E.; Hunt, H. R.; Mcdowell, J.; Ray, J. D.; Dissociation Constants of Alpha-Oxyhyponitrous Acid, *Inorg. Chem.*, 1963, 2, 649-650.
29. Dutton, A. S.; Fukuto, J. M.; Houk, K. N.; Mechanisms of HNO and NO Production from Angeli's Salt: Density Functional and CBS-QB3 Theory Predictions, *J. Am. Chem. Soc.*, 2004, 126, 3795-3800.
30. Fukuto, J. M.; Bartberger, M. D.; Dutton, A. S.; Paolocci, N.; Wink, D. A.; Houk, K. N.; The Physiological Chemistry and Biological Activity of Nitroxyl (HNO): The Neglected, Misunderstood, and Enigmatic Nitrogen Oxide, *Chem. Res. Toxicol.*, 2005, 18, 790-801.
31. Bonner, F. T.; Ravid, B.; Thermal Decomposition of Oxyhyponitrite (Sodium Trioxodinitrate(II)) in Aqueous Solution, *Inorg. Chem.*, 1975, 14, 558-563.
32. Wong, P. S.-Y.; Hyun, J.; Fukuto, J. M.; Shirota, F. N.; DeMaster, E. G.; Shoeman, D. W.; Nagasawa, H. T.; Reaction between *S*-Nitrosothiols and Thiols: Generation of Nitroxyl (HNO) and Subsequent Chemistry, *Biochemistry*, 1998, 37, 5362-5371. [Erratum, p18129].
33. Amatore, C.; Arbault, S.; Ducrocq, C.; Hu, S.; Tapsoba, I.; Angeli's Salt ($Na_2N_2O_3$) is a Precursor of HNO and NO: a Voltammetric Study of the Reactive Intermediates Released by Angeli's Salt Decomposition, *Chem. Med. Chem.*, 2007, 2, 898-903.
34. Miranda, K. M.; Yamada, K.-I.; Espey, M. G.; Thomas, D. D.; DeGraff, W.; Mitchell, J. B.; Krishna, M. C.; Colton, C. A.; Wink, D. A.; Further Evidence for Distinct Reactive Intermediates from Nitroxy and Peroxynitrite: Effects of Buffer Composition on the Chemistry of Angeli's Salt and Synthetic Peroxynitrite, *Arch. Biochem. Biophys.*, 2002, 401, 134-144.

